Original Article

Imatinib Mesylate-Incorporated Nanoparticle-Eluting Stent Attenuates In-Stent Neointimal Formation in Porcine Coronary Arteries

Seigo Masuda[1], Kaku Nakano[1], Kouta Funakoshi[1], Gang Zhao[2], Wei Meng[2], Satoshi Kimura[3], Tetsuya Matoba[1], Miho Miyagawa[1], Eiko Iwata[1], Kenji Sunagawa[1] and Kensuke Egashira[1]

[1]Department of Cardiovascular Medicine, Graduate School of Medical Sciences, Kyushu University, Fukuoka, Japan
[2]Department of Cardiovascular Medicine, 6th People's Hospital, Shanghai Jiatong University, Shanghai, China
[3]Department of Cardiovascular Surgery, Graduate School of Medical Sciences, Kyushu University, Fukuoka, Japan

Aim: The use of currently marketed drug-eluting stents (DES) presents safety concerns, including an increased risk for late thrombosis in the range of 0.6% per year in patients, including acute coronary syndrome, which is thought to result from delayed endothelial healing effects. A new DES system targeting vascular smooth muscle cells without adverse effects on endothelial cells is therefore needed. Platelet-derived growth factor (PDGF) plays a central role in the pathogenesis of restenosis; therefore, we hypothesized that imatinib mesylate (PDGF receptor tyrosine kinase inhibitor) encapsulated bioabsorbable polymeric nanoparticle (NP)-eluting stent attenuates in-stent neointima formation.
Methods: Effects of imatinib-incorporated NP-eluting stent on neointima formation and endothelial healing were examined in a pig coronary artery stent model. Effects of imatinib-NP were also examined in cultured cells.
Results: In a cultured cell study, imatinib-NP attenuated the proliferation of vascular smooth muscle cells associated with inhibition of the target molecule (phosphorylation of PDGF receptor-β), but showed no effect on endothelial proliferation. In a pig coronary artery stent model, imatinib-NP-eluting stent markedly attenuated in-stent neointima formation and stenosis by approximately 50% as assessed by angiographic, histopathological, and intravascular ultrasound imaging analyses. Imatinib-NP-eluting stent also attenuated MAP kinase activity, but did not affect inflammation and re-endothelialization.
Conclusion: These data suggest that suppression of neointima formation by a imatinib-NP-eluting stent holds promise as a molecular-targeting NP delivery system for preventing in-stent restenosis.

J Atheroscler Thromb, 2011; 18:1043-1053.

Key words; Nanotechnology, Drug delivery system, Restenosis, Stents, Smooth muscle cells

Introduction

Although polymer-coated drug-eluting stents (DES) can reduce restenosis and target-vessel revascularization to rates below 10% by its anti-proliferative effects on vascular smooth muscle cells (VSMC), increased risk of late in-stent thrombosis resulting in acute coronary syndrome (unstable angina, acute myocardial infarction and death) after the use of DES devices has become a major safety concern[1-3]. These adverse effects are thought to result mainly from delayed healing effects of the drugs or polymers on endothelial cells leading to impaired arterial healing processes (impaired endothelial regeneration, excessive inflammation, proliferation and fibrin deposition)[4-6]. Cell-specific molecular targeting against VSMC proliferation without negative effects on endothelial cells,

Address for correspondence: Kensuke Egashira, Department of Cardiovascular Medicine, Graduate School of Medical Science, Kyushu University, 3-1-1, Maidashi, Higashi-ku, Fukuoka 812-8582, Japan
E-mail: egashira@cardiol.med.kyushu-u.ac.jp
Received: January 20, 2011
Accepted for publication: July 1, 2011

therefore, is an essential requirement to develop more efficient and safer DES in the future.

Platelet-derived growth factor (PDGF), expressed by VSMC, plays a central role in the pathogenesis of restenosis. Mechanical forces, such as stent-induced overstretch, stimulate VSMC expression and release of PDGF in animals[7, 8] and humans[9, 10]. Imatinib mesylate is an inhibitor for c-Abl tyrosine kinase, c-Kit receptor kinase, and PDGF receptor tyrosine kinase[11, 12] and is approved for the treatment of patients with chronic myeloid leukemia. It has been shown that c-Kit-positive progenitor cells can differentiate into α-actin-positive VSMCs and may contribute to neointima formation[13]. It has also been reported that c-Abl tyrosine kinase is involved in angiotensin II-induced VSMC hypertrophy[14]. Imatinib is reported to be a significantly more potent inhibitor of VSMC proliferation than other inhibitors of PDGF receptor (AGL-2043), with $IC_{50} < 10$ nM[15]. In contrast, imatinib has little effect on vascular endothelial cell growth factor receptor tyrosine kinase or endothelial cell proliferation[15]. These data provide a rationale for the use of imatinib mesylate in the prevention of neointima formation associated with in-stent restenosis as a VSMC-specific molecular-targeting drug.

Prior studies have reported that systemic oral administration of imatinib inhibited balloon injury-induced neointima formation in rats[11] when dosages beyond the clinical norm were used (50 mg/kg per day). In contrast, imatinib had no effect on in-stent neointima formation in rabbits when administered at a clinically relevant dosage (10 mg/kg per day)[16]. Recent clinical studies in humans have detected no beneficial effects of the oral administration of imatinib (600 mg/day for 10 days)[17] on in-stent restenosis. These data suggest that systemic administration of imatinib at clinical dosages may not be sufficient to antagonize PDGF-induced vascular responses. Furthermore, it was reported the polymer-coated stents with imatinib (600 μg/stent) had no effect on neointima formation in a porcine coronary in-stent stenosis model[15]. This was probably because of unsuitable release characteristics of imatinib from polymer-coated stents. It is suggested that the present polymer coating DES technology is not useful for coating water-soluble drugs such as imatinib. Therefore, preventing in-stent restenosis via imatinib-mediated PDGF-R signaling blockade requires a new efficient drug delivery system. We previously succeeded in developing bioabsorbable polymeric nanoparticles (NP) formulated from the polymer poly (DL-lactide-co-glycolide) (PLGA)[18], and in formulating a NP-eluting stent by cation electrodeposition coating technology[19]. This NP-eluting stent system provided an effective means of delivering NP-incorporated drugs or genes that target intracellular proteins involved in the pathogenesis of in-stent neointima formation.

Therefore, we hypothesized that imatinib-NP-eluting stent can be an innovative therapeutic strategy for preventing in-stent neointima formation *in vivo*. We used a porcine coronary artery in-stent stenosis model and investigated whether imatinib-NP-eluting stent attenuates in-stent neointima formation without adverse effects on arterial healing processes *in vivo*.

Materials and Methods

Vascular Smooth Muscle Cell Proliferation Assay

Human coronary artery VSMCs (Lonza, Walkersville, MD, USA) were cultured and placed into 48-well culture plates (5000 cells per well; BD). Proliferation was stimulated by the addition of PDGF at 10 ng/mL (Sigma, Tokyo, Japan)[20]. Various concentration of imatinib (Novartis Pharma) at 0.1, 1, and 10 μM, imatinib-loaded PLGA NP (PLGA at 0.5 mg/mL containing imatinib at 10 μM), or vehicle alone was added to the wells, and four days later, the cells were fixed with methanol and a single observer counted the number of cells/plate.

Endothelial Cell Proliferation Assay

Human umbilical vein endothelial cells (HUVEC) were obtained, cultured, and used between passages 4 to 8[21]. Recombinant human VEGF165 (10 ng/mL; R&D) or PDGF at 10 ng/mL was added to the basal medium, and cells (7500 cells per well) were incubated in the presence or absence of imatinib, imatinib-NP, or vehicle for 4 days in 48-well culture plates. Cell count assay was performed as stated above.

Preparation of NP-Eluting Stents by Cationic Electrodeposition Coating Technology

A lactide/glycolide copolymer (PLGA) with an average molecular weight of 20,000 and a lactide to glycolide copolymer ratio of 75:25 (PLGA7520; Wako Pure Chemical Industries, Osaka, Japan) was used as wall material for the NP. Chitosan was used to coat the surface of PLGA NP. Polyvinylalcohol (PVA-403; Kuraray, Osaka, Japan) was used as a dispersing agent. PLGA NP incorporated with the fluorescent marker fluorescein isothiocyanate (FITC; Dojindo laboratories, Kumamoto, Japan) or with imatinib (purchased from a pharmacy) were prepared by a previously reported emulsion solvent diffusion method in purified water[19, 22, 23].

The mean particle size was analyzed by the light

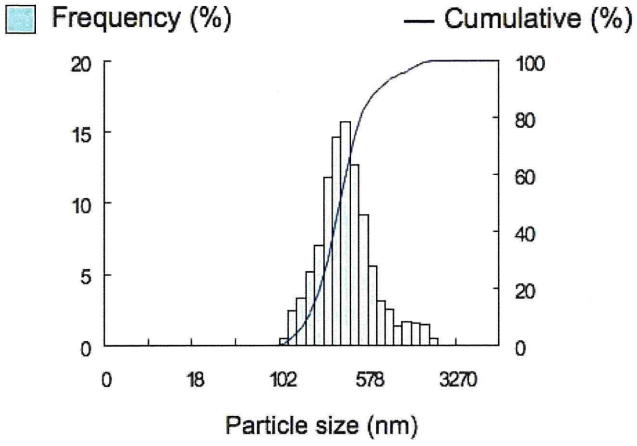

Fig. 1. Particle size distribution of imatinib-incorporated PLGA nanoparticles in water.

scattering method (Microtrack UPA150; Nikkiso, Tokyo, Japan). A sample of nanoparticulate suspension in distilled water was used for particle size analysis. The average diameter of FITC- and imatinib-incorporated NP was about 200 nm. Size distribution was similar between FITC-NP and imatinib-NP (see **Fig. 1**). FITC- and imatinib-encapsulated PLGA NP contained 5.0% (w/w) FITC and 8.3% (w/w) imatinib, respectively. The zeta potential of the NP as measured by Zetasizer Nano Z (Malverm, America) was +6.7 and +10.0 mV, respectively.

The 16 mm-long stainless-steel, balloon-expandable stents (Multilink) were ultrasonically cleaned in acetone, ethanol, and demineralized water. The cationic electrodeposited coating was prepared on cathodic stents in NP solution at a concentration of 5 g/L in distilled water with a current maintained between 2.0 and 10.0 mA by a direct current power supply (DC power supply; Nippon Stabilizer Co, Tokyo, Japan) for different periods under sterile conditions[19]. The coated stents were then rinsed with demineralized water and dried under a vacuum overnight. This electrodeposition coating procedure produced a coating of approximately 250 ± 40 μg of the polymer NP per stent and 21 ± 8 μg of imatinib per stent (n=12). The surface of some NP-coating stents were observed with scanning electron microscopy (JXM8600; JEOL, Tokyo, Japan).

Prior to experimental use, non-coated bare metal and NP-coated stents were mounted mechanically over the 3-mm balloon for implantation in the coronary artery. These balloon-mounted stent sets were sterilized using ethylene oxide.

Animal Preparation and Stent Implantation

All *in vivo* experiments were reviewed and approved by the Committee on Ethics in Animal Experiments, Kyushu University Faculty of Medicine, according to the Guidelines of the American Physiological Society. This study also conforms to the Guide for the Care and Use of Laboratory Animals published by the US National Institutes of Health (NIH Publication No. 85-23, revised 1996).

Domestic male pigs (Kyudo, Tosu, Japan; aged 2 to 3 months and weighing 25 to 30 kg) received oral aspirin (330 mg/day) and ticlopidine (200 mg/day) until euthanasia from 3 days before the stent implantation procedure. Animals were anesthetized with ketamine hydrochloride (15 mg/kg, IM) and pentobarbital (20 mg/kg, IV). They were then intubated and mechanically ventilated with room air. A preshaped Judkins catheter was inserted into the carotid artery and advanced to the orifice of the left coronary artery. After systemic heparinization (100 IU/kg) and intracoronary administration of nitroglycerin, coronary angiography of the left coronary artery was performed using contrast media (iopamidol 370®) in a left oblique view with an angiography system (Toshiba Medical, Tokyo, Japan). Animals were divided into 3 groups, which underwent deployment of either a non-coated bare metal stent (2 week; n=4 for Western blot analysis, 4 week; n=10 for angiographic, histopathological and intravascular ultrasound analyses), FITC-incorporated NP-eluting stents (4 week; n=10 for angiographic, histopathological and intravascular ultrasound analyses), or imatinib-incorporated NP-eluting stents (2 week; n=4 for Western blot analysis, 4 week; n=10 for angiographic, histopathological and intravascular ultrasound analyses), to either the left anterior descending (LAD) or the left circumflex coronary (LCx) arteries.

A segment with a mean coronary diameter of 2.5 mm was selected by using quantitative coronary angiography (Toshiba Medical, Tokyo, Japan) with a stent-to-artery ratio of approximately 1.1 to 1.2 (**Table 1**). A balloon catheter mounted with a stent was then advanced to the pre-selected coronary segments for deployment over a standard guidewire. The balloon catheter was inflated at 12 atm for 60 seconds once and thereafter deflated, and was then slowly withdrawn, leaving the stent in place.

Quantitative coronary angiography (Toshiba Medical, Tokyo, Japan) was performed before, immediately after, and 4 weeks after stent implantation to examine the coronary arterial diameter at stented and non-stented sites. An image of a Judkins catheter was used as the reference diameter. Arterial pressure, heart

rate, and ECG were continuously monitored and recorded on a recorder.

Intravascular Ultrasound

Intravascular ultrasound imaging (IVUS) was performed to assess the extent of neointima formation *in vivo* 4 weeks after stent implantation. Imaging was performed using a 40 MHz ultrasonic imaging catheter (Ultra cross; Boston Scientific, Boston, USA) and an automatic pullback device, and the studies were recorded on 1/2-inch high-resolution s-VHS tapes for off-line volumetric assessment. Because of the limited availability of IVUS probes, IVUS was performed 7 and 8 pigs in FITC-NP and imatinib-NP stent groups, respectively.

Histopathological Study

Four weeks after the coronary angiographic study, animals were euthanized with a lethal dose of sodium pentobarbital (40 mg/kg intravenously), and histological analysis was performed. The left coronary artery was perfused with 10% buffered formalin at 120 mm Hg and fixed for 24 hours. The stented artery segments were isolated and processed as described previously[24]: The segment was cut at the center of the stent and embedded in methyl methacrylate mixed with n-butyl methacrylate to allow for sectioning through the metal stent struts. Serial sections were stained with elastica van Gieson and with hematoxylin-eosin (HE). The neointimal area, the area within the internal elastic lamina (IEL), and the lumen area were measured by computerized morphometry, which was carried out by a single observer who was blinded to the experimental protocol. All images were captured by an Olympus microscope equipped with a digital camera (HC-2500) and were analyzed using Adobe Photoshop 6.0 and Scion Image 1.62 Software. The injury, inflammation, and re-endothelialization scores were determined at each strut site, and mean values were calculated for each stented segment[25].

Western Blot Analysis

For *in vitro* study, protein was extracted from cultured VSMC, and protein expression was analyzed using antibodies against human PDGF receptor-β (0.1 mg/mL; R&D Systems Inc.), phospho-PDGF receptor-β (0.5 mg/mL; R&D), or anti-actin (Sigma).

For *in vivo* study, animals were euthanized with a lethal dose of sodium pentobarbital (40 mg/kg intravenously) two weeks after stent implantation when the neointima was modestly formed, and Western blot analysis was performed. Protein was extracted from frozen arterial tissues excised from stented coronary arterial segments (LAD or LCx) and non-stented normal coronary arterial segments (right coronary artery). Cell extracts (20 μg) were resolved on 10% reducing SDS-PAGE gels and blotted onto nitrocellulose membranes (Bio-Rad, Hercules, CA). Protein expression was analyzed using antibodies against MAP kinase (ERK1/2) (0.5 mg/mL; R&D Systems Inc.), phosho-ERK1/2 (1:2000; Cell Signaling), or anti-actin (Sigma). Immune complexes were visualized with horseradish peroxidase-conjugated secondary antibodies (Pierce, Rockford, IL) using the ECL Plus system (Amersham Biosciences). Western blot analysis was performed with sequential antibodies and was detected with the ECL Detection Kit (Amersham).

Statistical Analysis

Data are expressed as the means ± SE. Statistical analysis of differences between two groups was performed with the unpaired t-test, and the statistical analysis of differences among three or more groups was assessed using ANOVA and multiple comparison tests. P values < 0.05 were considered significant.

Results

In vitro Effects of Imatinib on Proliferation of Vascular Smooth Muscle Cells and Endothelial Cells

We previously reported (1) the *in vitro* time course of FITC release from FITC-incorporated NP, and (2) highly efficient and stable delivery of NP into the cytoplasm of SMC and endothelial cells[19, 21, 26, 27]. In the present study, we examined *in vitro* effects of imatinib and imatinib-NP. As reported by others[15], imatinib attenuated the PDGF-induced proliferation of human coronary arterial SMC in a dose-dependent manner (**Fig. 2A**). Imatinib-NP also prevented the PDGF-induced responses of SMC. Western blot analysis showed that in human coronary artery SMC, both imatinib and imatinib-NP inhibited PDGF-induced phosphorylation of PDGF receptor-β in a dose-dependent manner (**Fig. 2B**). In contrast, neither imatinib nor imatinib-NP affected VEGF- and PDGF-induced proliferation of human endothelial cells (**Fig. 2C**).

Effects of Imatinib-NP-Eluting Stent on Neointima Formation 4 Weeks After Stent Implantation

Three animals (2 in control bare metal stent group and 1 in FITC-NP-eluting stent group) died suddenly between weeks 3 and 4; therefore, these animals were excluded from angiographic and histopathological analyses. These analyses were performed in 27

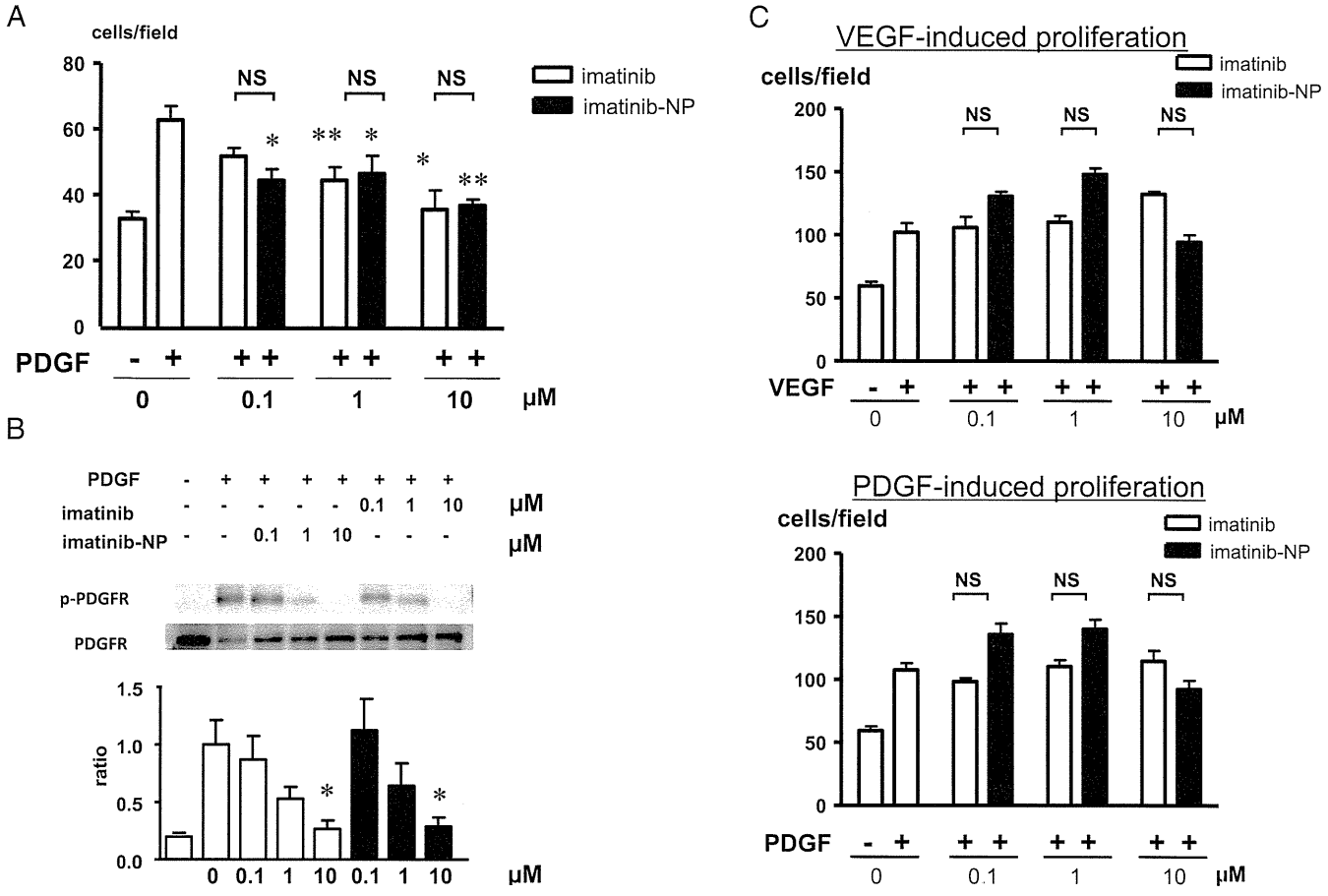

Fig. 2.

A, Effects of imatinib and imatinib-NP on PDGF-induced proliferation of human coronary artery SMCs. Data are the mean ± SEM ($n = 8$ each). $^{*}p < 0.001$ versus PDGF-induced response by two-way ANOVA and Dunnett's multiple comparison tests.
B, Effects of imatinib and imatinib-NP on PDGF-induced activation (phosphorylation) of PDGF receptor-β in human coronary artery SMC. Densitometric analysis of protein expression (p-PDGFR/PDGFR ratio) is also shown as a bar graph ($n = 5$ each). $^{*}p < 0.05$ versus the PDGF-induced response by one-way ANOVA and Dunnett's multiple comparison tests.
C, Effect of imatinib on the VEGF- and PDGF-induced proliferation of human umbilical vein endothelial cells ($n = 8$).

Table 1. Coronary artery diameter before, immediately after, and 4 weeks after stent implantation in porcine coronary artery

	Bare metal control stent ($n = 8$)	FITC-NP-eluting stent ($n = 9$)	imatinib-NP-eluting stent ($n = 10$)	p value
coronary diameter before stent implantation	2.21 ± 0.06	2.25 ± 0.05	2.32 ± 0.05	0.33
coronary diameter immediately after stent implantation	2.63 ± 0.08	2.65 ± 0.05	2.70 ± 0.04	0.70
stent-to-artery ratio immediately after stent implantation	1.19 ± 0.03	1.18 ± 0.03	1.17 ± 0.02	0.74
coronary diameter 4 weeks after stent implantation	1.48 ± 0.14	1.49 ± 0.12	2.06 ± 0.16	0.009

Data are the mean ± SEM. $^{*}p < 0.01$ versus coronary diameter before stent implantation, $^{\dagger}p < 0.01$ versus coronary diameter immediately after stent implantation, $^{\#}p < 0.01$ versus bare metal control stent group.

pigs (8 in control bare metal stent group, 9 in FITC-NP-eluting stent group, and 10 in imatinib-NP eluting stent group).

Quantitative coronary arteriography revealed that (1) there was no significant difference in the coronary diameter before and immediately after stent implantation and the stent-to-artery ratio among the 3 groups; and (2) the coronary diameter was less in

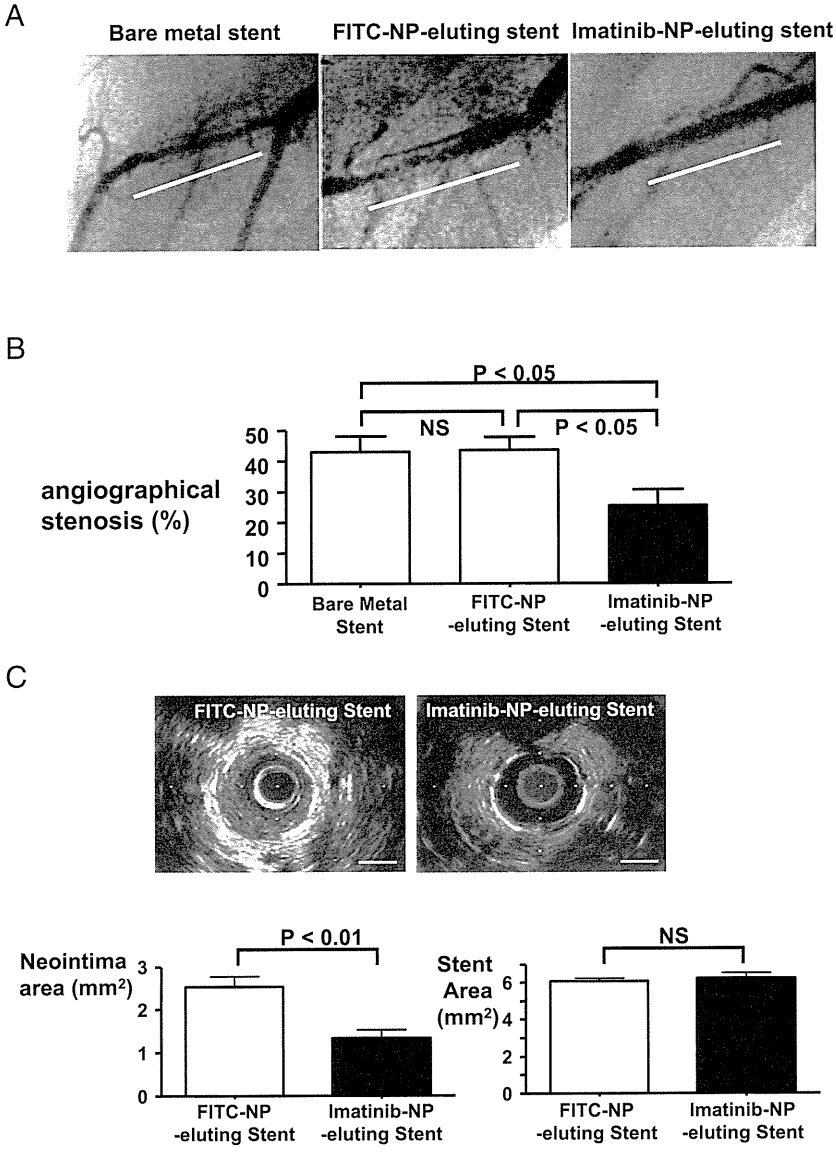

Fig. 3. Coronary arteriography and in-stent stenosis 4 weeks after stent implantation.

A, Representative coronary arteriographic images of stented segments in the left anterior descending coronary artery in bare metal, FITC-NP-eluting, and imatinib-NP-eluting stent groups. White bars in the images denote stented segments.
B, Angiographically-examined in-stent stenosis in bare metal ($n=8$), FITC-NP-eluting ($n=9$), and imatinib-NP-eluting ($n=10$) stent groups.
C, Intravascular ultrasound cross-section images and the summary of neointima formation (neointima area and stent area) in FITC-NP-eluting ($n=7$) and imatinib-NP-eluting ($n=8$) stent groups. Bar=1 mm.

the control bare metal and FITC-NP-eluting stent sites than in the imatinib-NP-eluting stent sites 4 weeks after stenting (**Table 1**). Thus, angiographically, in-stent stenosis was less in the imatinib-NP group than in the control and FITC-NP group (**Fig. 3A and B**).

Intravascular ultrasound imaging (IVUS) could be performed in FITC-NP ($n=7$) and imatinib-NP stent ($n=8$) groups, which demonstrated that the extent of neointima formation was significantly less at the imatinib-NP stent site than at the FITC-NP-stent site (**Fig. 3C**).

Histological analysis demonstrated that a signifi-

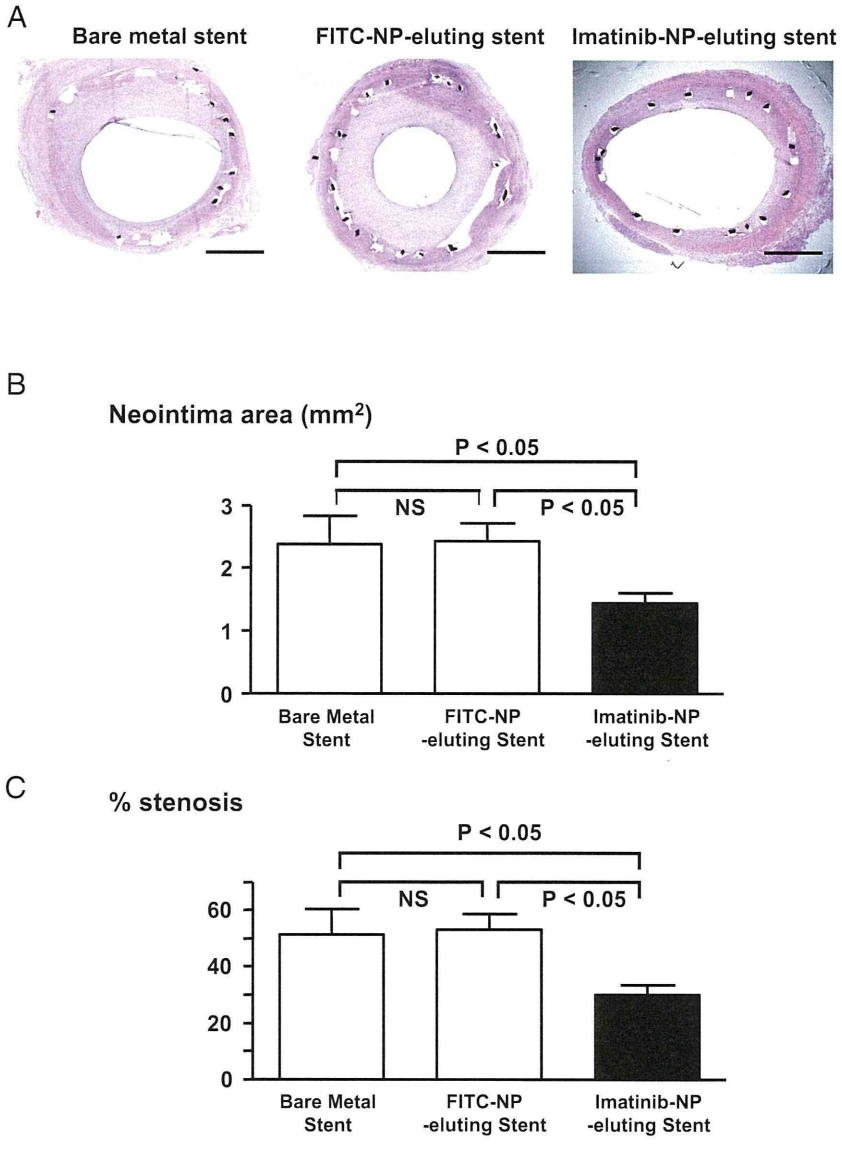

Fig. 4. Histopathological analysis of in-stent neointima formation 4 weeks after stent implantation.

A, Coronary artery cross-sections from the bare metal stent, FITC-NP-eluting stent, and the imatinib-NP-eluting stent groups. Tissue was stained with hematoxylin-eosin. Bar = 1 mm.

B, The neointima area at bare metal stents ($n = 8$), FITC-NP-eluting stents stents ($n = 9$), and the imatinib-NP-eluting stents ($n = 10$). NS = not significant. For statistical analysis, one-way ANOVA and Bonferroni's multiple comparison tests were performed.

C, The % stenosis [100 × (area of internal elastic lamia - neointima area)/area of internal elastic lamia] at bare metal stents, FITC-NP-eluting stents and the imatinib-NP-eluting stents. NS = not significant.

cant in-stent neointima formed similarly at the non-coated bare metal stent and FITC-NP-eluting stent sites. Quantitative analysis demonstrated a significant reduction in neointima formation at the imatinib-NP-eluting stent site (**Fig. 4**). In contrast, there were no significant differences in IEL and EEL areas among all 3 groups (**Table 2**). A semiquantitative histological scoring system demonstrated no significant difference in the injury score and inflammation score among the 3 groups (**Table 3**). Endothelial cell linings were

Table 2. Histopathological analysis of in-stent neointima formation 4 weeks after stent implantation in porcine coronary artery

	Bare metal control stent ($n=8$)	FITC-NP-eluting stent ($n=9$)	imatinib-NP-eluting stent ($n=10$)	p value
Area within the internal elastic lamina (IEL), mm^2	4.56 ± 0.11	4.54 ± 0.09	4.84 ± 0.14	0.13
Area within the external elastic lamina (EEL), mm^2	5.72 ± 0.18	5.76 ± 0.10	5.96 ± 0.14	0.40
Lumen area, mm^2	2.18 ± 0.38	2.11 ± 0.24	3.41 ± 0.23**	0.003

Data are the mean ± SEM. *$p<0.05$, **$p<0.01$ versus control bare metal stent.

Table 3. Re-endothelialization, injury score, and inflammation score 4 weeks after stenting

	Bare metal control stent ($n=8$)	FITC-NP-eluting stent ($n=9$)	imatinib-NP-eluting stent ($n=10$)	p value
Re-endothelialization score	3 ± 0	3 ± 0	3 ± 0	1.0
Injury score	1.75 ± 0.09	1.79 ± 0.09	1.88 ± 0.08	0.57
Inflammation score	1.70 ± 0.14	1.62 ± 0.08	1.75 ± 0.06	0.63

Data are the mean ± SEM.
The re-endothelialization score was defined as the extent of the circumference of the arterial lumen covered by endothelial cells and was scored from 1 to 3 (1=25%; 2=25% to 75%; 3 ≥75%)[23].
The injury score was determined at each strut site, and mean values were calculated for each stented segment[23]. In brief, a numeric value from 0 (no injury) to 3 (most injury) was assigned: 0=endothelial denudate, internal elastica lamina (IEL) intact; 1=IEL lacerated, media compressed, not lacerated; 2=IEL lacerated, media lacerated, external elastica lamina (EEL) compressed, not lacerated; and 3=media severely lacerated, EEL lacerated, adventitial may contain stent strut. The average injury score for each segment was calculated by dividing the sum of injury scores by the total number of struts in the examined section.
The inflammation score took into consideration the extent and density of the inflammatory infiltrate in each individual strut[23]. With regard to the inflammatory score for each individual strut, the grading is: 0=no inflammatory cells surrounding the strut; 1=light, noncircumferential inflammatory cells infiltrate surrounding the strut; 2=localized, moderate to dense cellular aggregate surrounding the strut noncircumferentially; and 3=circumferential dense inflammatory cells infiltration of the strut. The inflammatory score for each cross section was calculated in the same manner as for the injury score (sum of the individual inflammatory scores, divided by the number of struts in the examined section).

observed equally in the 3 groups (**Table 3**).

Effects of Imatinib-NP-Eluting Stent on Protein Expression of MAP Kinase *in vivo*

Western blot analysis was performed in another set of animals, which underwent deployment of both a bare metal stent and imatinib-NP-eluting stent to either LAD or LCx. On day 14 post-stenting, the neointima, and the media and adventitia were harvested. Protein expression of the phosphorylation of ERK was significantly less at the imatinib-NP-eluting stent site than at the bare metal stent site (**Fig. 5**). In contrast, no significant changes were found in phosphorylated ERK expression in the media and adventitia.

Discussion

We here report the first successful development of imatinib-NP-eluting stents with a newly invented cation electrodeposition coating technology. Importantly, this NP-mediated drug delivery platform is able to carry hydrophilic agents such as imatinib, which offers advantages over the current stent-coating technology. We here showed that (1) imatinib-NP caused the cell-specific targeting of VSMC proliferation associated with inhibition of the target molecules of imatinib (phosphorylation of PDGF receptor-β) *in vitro*; (2) imatinib-NP showed no negative effects on the proliferation of endothelial cells *in vitro*, and (3) imatinib-NP-eluting stent effectively attenuated in-stent stenosis (neointima formation) by about 50% as compared to bare metal stents and FITC-NP eluting stents in porcine coronary arteries without apparent negative effects on the endothelial healing process *in vivo*.

We and others previously showed that (1) the PLGA NP was taken up by cultured SMC mainly via endocytosis, and retained stably in the intracellular space[18, 19, 21, 26, 28]. It is likely that after cellular or tissue uptake of NP, NP slowly releases the encapsulated drug (imatinib in this case) into the cytoplasm or

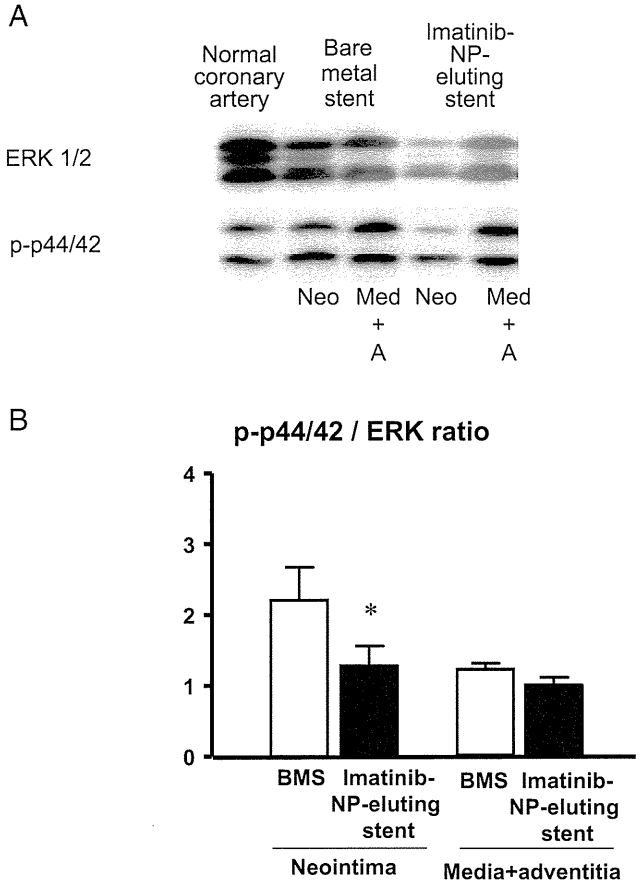

Fig. 5. Protein expression of MAP kinase (p-ERK1/2/ERK 1/2) 14 days after stenting.

A, Photographs of immunoblots of tissues from neointima (neo) and media plus adventitia (Med + A) from normal coronary artery sites (NCA), bare metal stent sites, and imatinib-NP-eluting stent sites.

B, Densitometric analysis of protein expression ($n = 4$ each). $^*p < 0.05$ versus bare metal stent site.

extracellular space as PLGA is hydrolyzed, resulting in prolonged delivery of imatinib into the stented coronary artery. In this regard, we recently reported that this bioabsorbable polymeric NP-eluting stent system has unique aspects in vascular compatibility and an efficient drug delivery system (stable delivery of NP into the neointima and medial layers until day 28 after deployment of a NP-eluting stent), compared to a dip-coated polymer-eluting stent[19].

In contrast to our present findings, prior studies failed to demonstrate the inhibitory effect of imatinib on in-stent neointima formation in rabbits (oral administration at 10 mg/kg per day for 6 weeks)[16], pigs (600 μg/stent)[15], and patients (oral administration at 600 mg/body per day for 10 days)[17]. The estimated dose of imatinib loaded on our NP-eluting stent was 21 ± 8 μg/stent, which is markedly lower than the doses used in these prior studies; therefore, it is likely that the inhibition of in-stent neointima formation is mediated by slower release and longer retention of imatinib at the imatinib-NP-eluting stent site in this porcine coronary artery model. To confirm this hypothesis, we tried to measure local tissue concentrations of imatinib immediately after and 6 hours after deployment of a imatinib-NP-eluting stent by the HPLC system as a preliminary experiment, which was under the limit of detection (1 ng/mL). Local concentrations of imatinib after deployment of imatinib-NP-eluting stent are unclear; however, our present data (**Fig. 5**) demonstrated that the attenuation of in-stent neointima formation by an imatinib-NP-eluting stent was associated with inhibition of the downstream signal of PDGF receptor (ERK) *in vivo*. Therefore, our present data provide evidence that PDGF receptor signaling blockade by an imatinib-NP-eluting stent may be a promising means for preventing in-stent neointima formation *in vivo*.

An impaired arterial healing process has been demonstrated to be a major histopathological feature in arteries exposed to currently marketed DES in experimental animals[29, 30] and in humans[4-6]. In this study, neither FITC- nor imatinib-NP-eluting stents had apparent effects on inflammation, injury, and re-endothelialization in porcine coronary arteries *in vivo*, suggesting that this NP-eluting stent system may not impair the healing process and endothelial regeneration in this model. Collectively, these data on vascular compatibility support the notion that this bioabsorbable PLGA NP-eluting stent system could be applied to human subjects. One limitation of this interpretation is that we did not compare delayed endothelial healing effects between our NP-eluting stent and current DES devices. In this respect, we do not know whether this approach may have an advantage over currently marketed first-generation DES devices. Future studies are needed to prove this point. Another limitation is that this study was performed in normal pigs without pre-existing atherosclerotic coronary lesions, although this porcine coronary artery model is regarded as an appropriate and standard preclinical study model[31]. A long-term efficacy study is also needed.

We and others have reported that monocyte-mediated inflammation induced by monocyte chemoattractant protein-1 (MCP-1) plays a central role in the pathogenesis of neointima formation[24, 32-36] and in atherogenesis[37, 38]. If imatinib and anti-MCP treatment exert their effects through different pathways, it would be interesting to examine whether combined

blockade of PDGF-R and MCP-1 would have additive inhibitory effects on in-stent stenosis.

In conclusion, blockade of PDGF signaling by imatinib-NP inhibited the proliferation of VSMC with no adverse effects on endothelial cells *in vitro*, and an imatinib-NP-eluting stent attenuated in-stent neointimal formation in porcine coronary arteries *in vivo*. This molecular-targeting NP-eluting stent system may be an innovative platform for delivering agents that target future diagnosis and treatment of atherosclerotic vascular disease.

Funding Sources

This study was supported by Grants-in-Aid for Scientific Research (19390216, 19650134) from the Ministry of Education, Science, and Culture, Tokyo, Japan, by Health Science Research Grants (Research on Translational Research and Nanomedicine) from the Ministry of Health Labor and Welfare, Tokyo, Japan, and by the Program for Promotion of Fundamental Studies in Health Sciences of the Organization for Pharmaceutical Safety and Research, Tokyo, Japan.

Disclosures

Dr. Egashira hold a patent on the results reported in the present study. The remaining authors report no conflicts.

References

1) Laskey WK, Yancy CW, Maisel WH: Thrombosis in coronary drug-eluting stents: Report from the meeting of the circulatory system medical devices advisory panel of the food and drug administration center for devices and radiologic health, december 7-8, 2006. Circulation, 2007; 115: 2352-2357
2) Serruys PW, Kutryk MJ, Ong AT: Coronary-artery stents. N Engl J Med, 2006; 354: 483-495
3) Shuchman M: Trading restenosis for thrombosis? New questions about drug-eluting stents. N Engl J Med, 2006; 355: 1949-1952
4) Luscher TF, Steffel J, Eberli FR, Joner M, Nakazawa G, Tanner FC, Virmani R: Drug-eluting stent and coronary thrombosis: Biological mechanisms and clinical implications. Circulation, 2007; 115: 1051-1058
5) Finn AV, Nakazawa G, Joner M, Kolodgie FD, Mont EK, Gold HK, Virmani R: Vascular responses to drug eluting stents. Importance of delayed healing. Arterioscler Thromb Vasc Biol, 2007
6) Finn AV, Joner M, Nakazawa G, Kolodgie F, Newell J, John MC, Gold HK, Virmani R: Pathological correlates of late drug-eluting stent thrombosis: Strut coverage as a marker of endothelialization. Circulation, 2007; 115: 2435-2441
7) Nakano K, Egashira K, Ohtani K, Zhao G, Funakoshi K, Ihara Y, Sunagawa K: Catheter-based adenovirus-mediated anti-monocyte chemoattractant gene therapy attenuates in-stent neointima formation in cynomolgus monkeys. Atherosclerosis, 2006
8) Shibata M, Suzuki H, Nakatani M, Koba S, Geshi E, Katagiri T, Takeyama Y: The involvement of vascular endothelial growth factor and flt-1 in the process of neointimal proliferation in pig coronary arteries following stent implantation. Histochem Cell Biol, 2001; 116: 471-481
9) Ueda M, Becker AE, Kasayuki N, Kojima A, Morita Y, Tanaka S: In situ detection of platelet-derived growth factor-a and -b chain mrna in human coronary arteries after percutaneous transluminal coronary angioplasty. Am J Pathol, 1996; 149: 831-843
10) Nakagawa M, Naruko T, Ikura Y, Komatsu R, Iwasa Y, Kitabayashi C, Inoue T, Itoh A, Yoshiyama M, Ueda M: A decline in platelet activation and inflammatory cell infiltration is associated with the phenotypic redifferentiation of neointimal smooth muscle cells after bare-metal stent implantation in acute coronary syndrome. J Atheroscler Thromb, 2010; 17: 675-687
11) Myllarniemi M, Frosen J, Calderon Ramirez LG, Buchdunger E, Lemstrom K, Hayry P: Selective tyrosine kinase inhibitor for the platelet-derived growth factor receptor in vitro inhibits smooth muscle cell proliferation after reinjury of arterial intima in vivo. Cardiovasc Drugs Ther, 1999; 13: 159-168
12) Savage DG, Antman KH: Imatinib mesylate--a new oral targeted therapy. N Engl J Med, 2002; 346: 683-693
13) Sata M, Saiura A, Kunisato A, Tojo A, Okada S, Tokuhisa T, Hirai H, Makuuchi M, Hirata Y, Nagai R: Hematopoietic stem cells differentiate into vascular cells that participate in the pathogenesis of atherosclerosis. Nat Med, 2002; 8: 403-409
14) Ushio-Fukai M, Zuo L, Ikeda S, Tojo T, Patrushev NA, Alexander RW: Cabl tyrosine kinase mediates reactive oxygen species- and caveolin-dependent at1 receptor signaling in vascular smooth muscle: Role in vascular hypertrophy. Circ Res, 2005; 97: 829-836
15) Hacker TA, Griffin MO, Guttormsen B, Stoker S, Wolff MR: Platelet-derived growth factor receptor antagonist sti571 (imatinib mesylate) inhibits human vascular smooth muscle proliferation and migration in vitro but not in vivo. J Invasive Cardiol, 2007; 19: 269-274
16) Leppanen O, Rutanen J, Hiltunen MO, Rissanen TT, Turunen MP, Sjoblom T, Bruggen J, Backstrom G, Carlsson M, Buchdunger E, Bergqvist D, Alitalo K, Heldin CH, Ostman A, Yla-Herttuala S: Oral imatinib mesylate (sti571/gleevec) improves the efficacy of local intravascular vascular endothelial growth factor-c gene transfer in reducing neointimal growth in hypercholesterolemic rabbits. Circulation, 2004; 109: 1140-1146
17) Zohlnhofer D, Hausleiter J, Kastrati A, Mehilli J, Goos C, Schuhlen H, Pache J, Pogatsa-Murray G, Heemann U, Dirschinger J, Schomig A: A randomized, double-blind, placebo-controlled trial on restenosis prevention by the receptor tyrosine kinase inhibitor imatinib. J Am Coll Cardiol, 2005; 46: 1999-2003

18) Yamamoto H, Kuno Y, Sugimoto S, Takeuchi H, Kawashima Y: Surface-modified plga nanosphere with chitosan improved pulmonary delivery of calcitonin by mucoadhesion and opening of the intercellular tight junctions. J Control Release, 2005; 102: 373-381
19) Nakano K, Egashira K, Masuda S, Funakoshi K, Zhao G, Kimura S, Matoba T, Sueishi K, Endo Y, Kawashima Y, Hara K, Tsujimoto H, Tominaga R, Sunagawa K: Formulation of nanoparticle-eluting stents by a cationic electrodeposition coating technology efficient nano-drug delivery via bioabsorbable polymeric nanoparticle-eluting stents in porcine coronary arteries. Jacc, 2009; 2: 277-283
20) Nakano K, Egashira K, Tada H, Kohjimoto Y, Hirouchi Y, Kitajima SI, Endo Y, Li XH, Sunagawa K: A third-generation, long-acting, dihydropyridine calcium antagonist, azelnidipine, attenuates stent-associated neointimal formation in non-human primates. J Hypertens, 2006; 24: 1881-1889
21) Kubo M, Egashira K, Inoue T, Koga J, Oda S, Chen L, Nakano K, Matoba T, Kawashima Y, Hara K, Tsujimoto H, Sueishi K, Tominaga R, Sunagawa K: Therapeutic neovascularization by nanotechnology-mediated cell-selective delivery of pitavastatin into the vascular endothelium. Arterioscler Thromb Vasc Biol, 2009; 29: 796-801
22) Murakami H, Kobayashi M, Takeuchi H, Kawashima Y: Preparation of poly(DL-lactide-co-glycolide) nanoparticles by modified spontaneous emulsification solvent diffusion method. International journal of pharmaceutics, 1999; 187: 143-152
23) Kawashima Y, Yamamoto H, Takeuchi H, Hino T, Niwa T: Properties of a peptide containing DL-lactide/glycolide copolymer nanospheres prepared by novel emulsion solvent diffusion methods. Eur J Pharm Biopharm, 1998; 45: 41-48
24) Ohtani K, Usui M, Nakano K, Kohjimoto Y, Kitajima S, Hirouchi Y, Li XH, Kitamoto S, Takeshita A, Egashira K: Antimonocyte chemoattractant protein-1 gene therapy reduces experimental in-stent restenosis in hypercholesterolemic rabbits and monkeys. Gene Ther, 2004; 11: 1273-1282
25) Schwartz RS, Huber KC, Murphy JG, Edwards WD, Camrud AR, Vlietstra RE, Holmes DR: Restenosis and the proportional neointimal response to coronary artery injury: Results in a porcine model. J Am Coll Cardiol, 1992; 19: 267-274
26) Kimura S, Egashira K, Nakano K, Iwata E, Miyagawa M, Tsujimoto H, Hara K, Kawashima Y, Tominaga R, Sunagawa K: Local delivery of imatinib mesylate (sti571)-incorporated nanoparticle ex vivo suppresses vein graft neointima formation. Circulation, 2008; 118: S65-70
27) Kimura S, Egashira K, Chen L, Nakano K, Iwata E, Miyagawa M, Tsujimoto H, Hara K, Morishita R, Sueishi K, Tominaga R, Sunagawa K: Nanoparticle-mediated delivery of nuclear factor kappab decoy into lungs ameliorates monocrotaline-induced pulmonary arterial hypertension. Hypertension, 2009; 53: 877-883
28) Panyam J, Zhou WZ, Prabha S, Sahoo SK, Labhasetwar V: Rapid endo-lysosomal escape of poly (dl-lactide-co-glycolide) nanoparticles: Implications for drug and gene delivery. Faseb J, 2002; 16: 1217-1226
29) van der Giessen WJ, Lincoff AM, Schwartz RS, van Beusekom HM, Serruys PW, Holmes DR Jr, Ellis SG, Topol EJ: Marked inflammatory sequelae to implantation of biodegradable and nonbiodegradable polymers in porcine coronary arteries. Circulation, 1996; 94: 1690-1697
30) Lincoff AM, Furst JG, Ellis SG, Tuch RJ, Topol EJ: Sustained local delivery of dexamethasone by a novel intravascular eluting stent to prevent restenosis in the porcine coronary injury model. J Am Coll Cardiol, 1997; 29: 808-816
31) Schwartz RS, Edelman ER, Carter A, Chronos N, Rogers C, Robinson KA, Waksman R, Weinberger J, Wilensky RL, Jensen DN, Zuckerman BD, Virmani R: Drug-eluting stents in preclinical studies: Recommended evaluation from a consensus group. Circulation, 2002; 106: 1867-1873
32) Usui M, Egashira K, Ohtani K, Kataoka C, Ishibashi M, Hiasa K, Katoh M, Zhao Q, Kitamoto S, Takeshita A: Anti-monocyte chemoattractant protein-1 gene therapy inhibits restenotic changes (neointimal hyperplasia) after balloon injury in rats and monkeys. Faseb J, 2002; 16: 1838-1840
33) Egashira K, Zhao Q, Kataoka C, Ohtani K, Usui M, Charo IF, Nishida K, Inoue S, Katoh M, Ichiki T, Takeshita A: Importance of monocyte chemoattractant protein-1 pathway in neointimal hyperplasia after periarterial injury in mice and monkeys. Circ Res, 2002; 90: 1167-1172
34) Egashira K: Molecular mechanisms mediating inflammation in vascular disease: Special reference to monocyte chemoattractant protein-1. Hypertension, 2003; 41: 834-841
35) Egashira K, Nakano K, Ohtani K, Funakoshi K, Zhao G, Ihara Y, Koga J, Kimura S, Tominaga R, Sunagawa K: Local delivery of anti-monocyte chemoattractant protein-1 by gene-eluting stents attenuates in-stent stenosis in rabbits and monkeys. Arterioscler Thromb Vasc Biol, 2007; 27: 2563-2568
36) Kitamoto S, Egashira K: Gene therapy targeting monocyte chemoattractant protein-1 for vascular disease. J Atheroscler Thromb, 2002; 9: 261-265
37) Ni W, Egashira K, Kitamoto S, Kataoka C, Koyanagi M, Inoue S, Imaizumi K, Akiyama C, Nishida Ki K, Takeshita A: New anti-monocyte chemoattractant protein-1 gene therapy attenuates atherosclerosis in apolipoprotein e-knockout mice. Circulation, 2001; 103: 2096-2101
38) Inoue S, Egashira K, Ni W, Kitamoto S, Usui M, Otani K, Ishibashi M, Hiasa K, Nishida K, Takeshita A: Anti-monocyte chemoattractant protein-1 gene therapy limits progression and destabilization of established atherosclerosis in apolipoprotein e-knockout mice. Circulation, 2002; 106: 2700-2706

Inhibition of Prolyl Hydroxylase Domain-Containing Protein Downregulates Vascular Angiotensin II Type 1 Receptor

Hirohide Matsuura, Toshihiro Ichiki, Jiro Ikeda, Kotaro Takeda, Ryohei Miyazaki, Toru Hashimoto, Eriko Narabayashi, Shiro Kitamoto, Tomotake Tokunou, Kenji Sunagawa

See Editorial Commentary, pp 354–355

Abstract—Inhibition of prolyl hydroxylase domain-containing protein (PHD) by hypoxia stabilizes hypoxia-inducible factor 1 and increases the expression of target genes, such as vascular endothelial growth factor. Although the systemic renin-angiotensin system is activated by hypoxia, the role of PHD in the regulation of the renin-angiotensin system remains unknown. We examined the effect of PHD inhibition on the expression of angiotensin II type 1 receptor (AT_1R). Hypoxia, cobalt chloride, and dimethyloxalylglycine, all known to inhibit PHD, reduced AT_1R expression in vascular smooth muscle cells. Knockdown of PHD2, a major isoform of PHDs, by RNA interference also reduced AT_1R expression. Cobalt chloride diminished angiotensin II–induced extracellular signal–regulated kinase phosphorylation. Cobalt chloride decreased AT_1R mRNA through transcriptional and posttranscriptional mechanisms. Oral administration of cobalt chloride (14 mg/kg per day) to C57BL/6J mice receiving angiotensin II infusion (490 ng/kg per minute) for 4 weeks significantly attenuated perivascular fibrosis of the coronary arteries without affecting blood pressure level. These data suggest that PHD inhibition may be beneficial for the treatment of cardiovascular diseases by inhibiting renin-angiotensin system via AT_1R downregulation. (***Hypertension.*** **2011;58:386-393.)** • **Online Data Supplement**

Key Words: angiotensin II type 1 receptor ■ renin angiotensin system ■ prolyl hydroxylase domain-containing protein ■ vascular remodeling

Renin-angiotensin system (RAS) physiologically and pathophysiologically plays a pivotal role in the cardiovascular system. RAS modulates blood pressure, fluid and electrolyte homeostasis, and neuronal function.[1] RAS is also critical for the pathogenesis of cardiovascular diseases, such as hypertension, atherosclerosis, ischemic heart disease, and congestive heart failure.[2] Angiotensin II (Ang II), the primary active circulating component of the RAS, is a multifunctional hormone responsible for many cellular processes, such as inflammation, fibrosis, migration, proliferation, hypertrophy, and apoptosis, resulting in the cardiovascular remodeling.[3] The effects of Ang II are mediated by Ang II receptors, and 2 distinct isoforms of 7-transmembrane, G protein-coupled receptors have ever been cloned, Ang II type 1 receptor (AT_1R)[4] and Ang II type 2 receptor.[5] It is generally accepted that AT_1R mainly contributes to the progression of cardiovascular diseases. Indeed, many large-scale randomized clinical trials showed the beneficial effects of AT_1R antagonists in the treatment of cardiovascular diseases.[6]

Cardiovascular diseases are intimately related to the reduced oxygen concentration state (hypoxia). Cardiomyocytes in ischemic heart disease, peripheral organs in heart failure, ischemic limb in arteriosclerosis obliterans, and the brain in cerebral infarction are subject to hypoxia. Recently, it was reported that hypoxia activates both circulating and local RAS.[7,8]

Hypoxia-inducible factor 1 (HIF-1) is a key transcription factor that plays a crucial role in the cellular adaptive response to hypoxia, such as erythrocytosis, glycolysis, and angiogenesis.[9] HIF-1 is a heterodimeric transcription factor composed of an O_2-regulated subunit HIF-1α and a constitutively expressed subunit HIF-1β.[10]

Expression of HIF-1α is negatively regulated by prolyl hydroxylase domain-containing protein (PHD). PHD mediates O_2-dependent hydroxylation of proline residue of HIF-1α, which triggers subsequent ubiquitination and proteasomal degradation of HIF-1α.[11] The PHD subfamily of 2-oxoglutarate/Fe^{2+}–dependent dioxygenases includes 3 isoforms (PHD1, PHD2, and PHD3). PHD2 is expressed more abundantly than other isoforms and is responsible for hypoxic response.[12] Hypoxia inhibits PHD activity, which stabilizes HIF-1α, resulting in the accumulation of HIF-1 in the nucleus and activation of expression of target genes such as vascular endothelial growth factor (VEGF) and phosphoglycerate kinase 1. In addition to

Received November 12, 2010; first decision November 25, 2010; revision accepted July 5, 2011.

From the Departments of Cardiovascular Medicine (H.M., T.I., J.I., R.M., T.H., E.N., S.K., T.T., K.S.) and Advanced Therapeutics for Cardiovascular Diseases (T.I., K.T., S.K.), Kyushu University Graduate School of Medical Sciences, Fukuoka, Japan.

Correspondence to Toshihiro Ichiki, Department of Cardiovascular Medicine, Kyushu University Graduate School of Medical Sciences, 3-1-1 Maidashi, Higashi-ku, 812-8582 Fukuoka, Japan. E-mail ichiki@cardiol.med.kyushu-u.ac.jp

Hypertension **is available at http://hyper.ahajournals.org** **DOI: 10.1161/HYPERTENSIONAHA.110.167106**

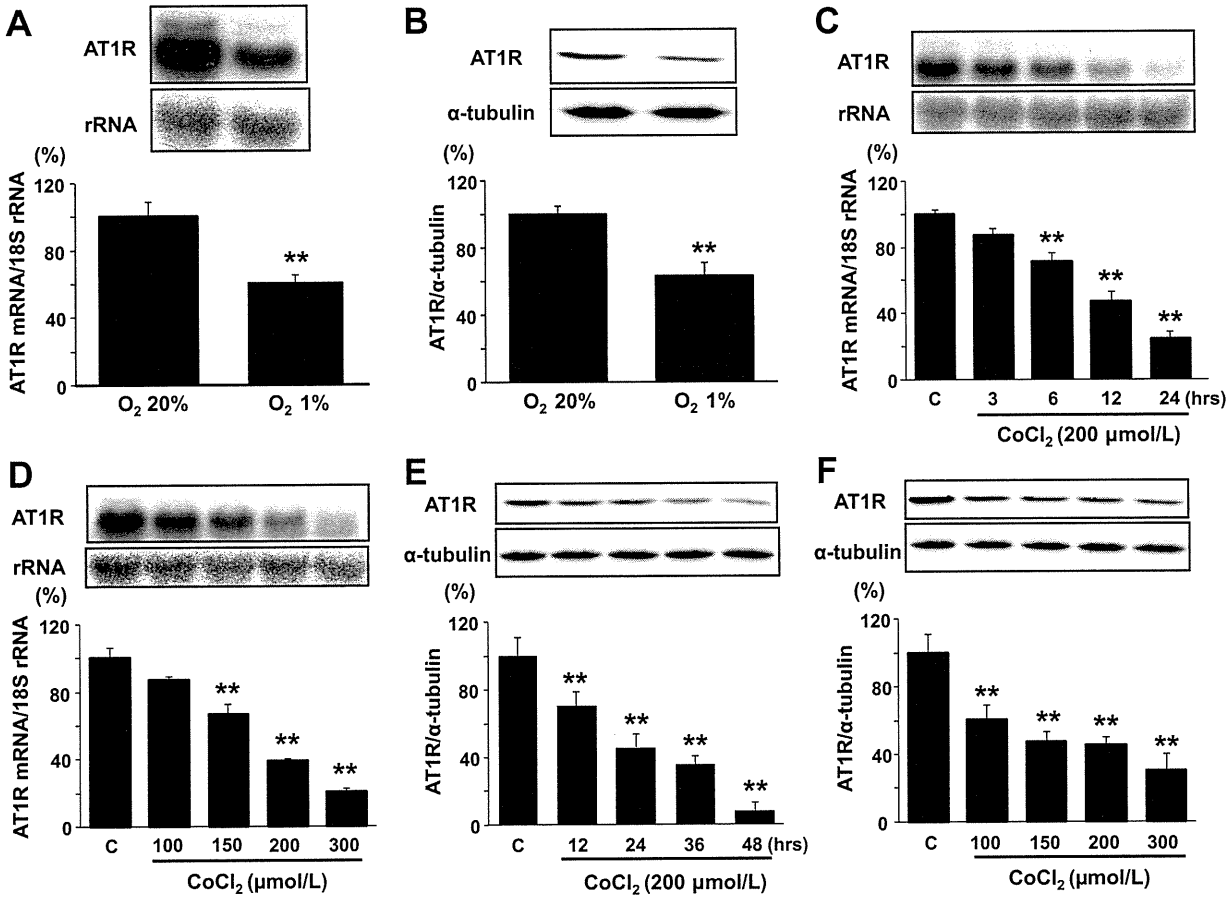

Figure 1. Hypoxia and cobalt chloride ($CoCl_2$) suppressed angiotensin II type 1 receptor (AT_1R) expression. **A** and **B**, Vascular smooth muscle cells (VSMCs) were incubated for 24 hours under normoxia (O_2 20%) or hypoxia (O_2 1%; n=4). **C**, and **E**, VSMCs were incubated with $CoCl_2$ (200 μmol/L) for varying periods as indicated in the figure (n=4). **D** and **F**, VSMCs were incubated with $CoCl_2$ at varying concentrations as indicated in the figure for 24 (for mRNA), and 48 hours (for protein), respectively (n=4). **A**, **C**, and **D**, Total RNA was isolated, and the expression of AT_1R mRNA and 18S rRNA was determined by Northern blot analysis. **B**, **E**, and **F**, Expression of AT_1R and α-tubulin protein was detected by Western blot analysis. The ratio of AT_1R/18S rRNA and the ratio of AT1R/α-tubulin are shown in the bar graph. Values (mean±SEM) are expressed as a percentage of culture at 20% O_2 concentration (100%) or control culture (C). *P<0.05, **P<0.01 vs O_2 20% or control.

hypoxia, cobalt chloride ($CoCl_2$) and dimethyloxalylglycine (DMOG) also inhibit PHD and stabilize HIF-1. Therefore, they are often referred to hypoxia mimetics.[13]

Although systemic RAS is activated by hypoxia,[7,8] the role of PHD in the regulation of RAS remains uncertain. In the present study, we examined whether PHD inhibition affects AT_1R expression and the Ang II signaling pathway in the vascular smooth muscle cell (VSMC) and vascular remodeling process.

Materials and Methods

To clarify the effect of PHD inhibition on vascular AT_1R expression, VSMCs from the thoracic aorta of Sprague-Dawley rats, which exclusively express AT_1R, were exposed to hypoxia, incubated with various PHD inhibitors ($CoCl_2$ and DMOG), or transfected with PHD2-specific small interfering RNA (siRNA). Expression of AT_1R, VEGF, and phosphoglycerate kinase 1 mRNA was examined by Northern blot analysis or quantitative RT-PCR. Expression of AT_1R, PHD2, and HIF-1α protein and extracellular signal–regulated kinase (ERK) phosphorylation was examined by Western blot analysis. Promoter activity was examined by luciferase assay. Cell viability was evaluated by trypan blue assay.

Nine-week–old male C57BL/6J mice were allocated into the following 4 groups: (1) control; (2) Ang II; (3) $CoCl_2$; and (4) Ang II+$CoCl_2$. In the Ang II group, 490 ng/kg per minute of Ang II was infused IP. $CoCl_2$ dissolved in water at 0.01% was administered ad libitum. Body weight, heart rate, and systolic blood pressure were measured. After 4 weeks, the perivascular fibrosis area of the small coronary arteries and the expression of AT_1R protein in the aorta were examined. Renin mRNA of the kidney and angiotensin-converting enzyme and Ang II type 2 receptor mRNA of the aorta were examined by real-time quantitative PCR. Serum angiotensinogen was examined by ELISA.

Statistical analysis was performed using a Student t test for the comparison of 2 groups. One-way ANOVA with Fishers post hoc test was used for multiple comparisons. The experiment indicated in Figure 3C was statistically analyzed by a 2-way ANOVA. Detailed information of materials and methods used in this study is available in the online Data Supplement (please see http://hyper.ahajournals.org).

Results

PHD Inhibition Suppressed AT_1R Expression in Rat VSMCs

Hypoxia (O_2 1%; 24 hours) reduced AT_1R mRNA and protein expression (Figure 1A and 1B). Hypoxia increased

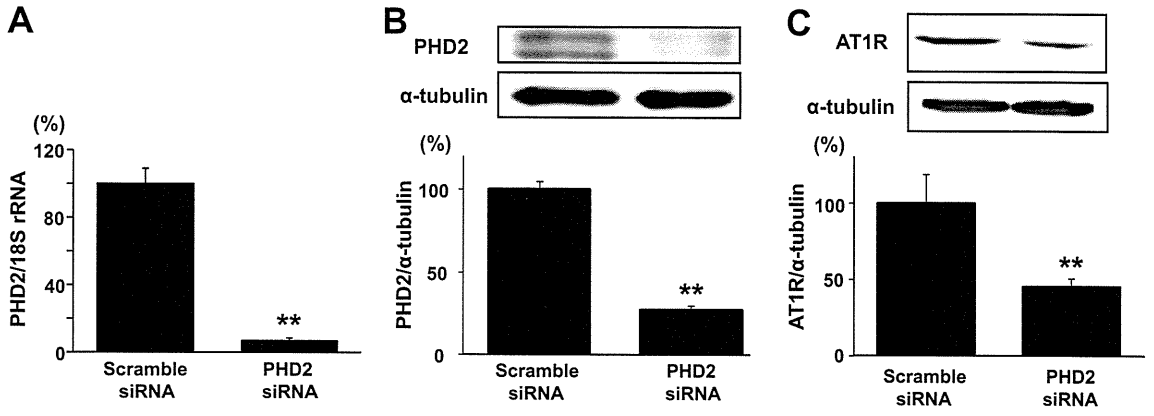

Figure 2. Knockdown of prolyl hydroxylase domain-containing protein (PHD) 2 suppressed angiotensin II type 1 receptor (AT_1R) expression. **A** through **C**, Vascular smooth muscle cells (VSMCs) were transfected with scramble small interfering RNA (siRNA) or PHD2-specific siRNA (n=3). After 72 hours, expression of PHD2 and 18S rRNA mRNA and expression of PHD2, AT_1R, and α-tubulin protein were determined by real-time quantitative PCR and Western blot analysis, respectively. **A**, The ratio of PHD2 mRNA/18S rRNA is shown in the bar graph. **B** and **C**, The ratio of PHD2 or AT_1R to α-tubulin is shown in the bar graph. Values (mean±SEM) are expressed as a percentage of scramble siRNA (100%). $^{**}P<0.01$ vs scramble siRNA.

expression of nuclear HIF-1α protein and mRNA expression of VEGF, its target gene, was also increased (Figure S1A and S2A, available in the online Data Supplement). Hypoxia (O_2 1%) increased hypoxia response element (HRE)–driven promoter activity measured by luciferase assay to 208.8±41.1% (Figure S3A). We then examined the effect of $CoCl_2$, one of the hypoxia mimetics, on AT_1R expression. Incubation of VSMCs with $CoCl_2$ (200 μmol/L) for varying time periods significantly reduced the expression level of AT_1R mRNA and significantly increased the expression level of VEGF mRNA in a time-dependent manner (Figures 1C and S2B). Incubation of VSMCs with varying concentrations of $CoCl_2$ resulted in dose-dependent downregulation of AT_1R mRNA and upregulation of VEGF mRNA (Figures 1D and S2C). $CoCl_2$ also increased nuclear HIF-1α expression and dose-dependently increased HRE-driven promoter activity (Figures S1A and S3B). These data indicate that $CoCl_2$ increased HIF-1. $CoCl_2$ induced AT_1R protein downregulation in a time- and dose-dependent manner (Figure 1E and 1F). DMOG, another PHD inhibitor, also downregulated AT_1R protein expression in a time- and dose-dependent manner (Figure S4A and S4B). Treatment of cells with control vehicle did not affect the expression of AT_1R protein at each time point (Figure S5A and S5B). To exclude a possible toxic effect of hypoxia, $CoCl_2$, and DMOG on VSMCs, we assessed the cell viability by trypan blue staining. Incubation of VSMCs under hypoxia (O_2 1%), with $CoCl_2$ (200 μmol/L) or with DMOG (1.0 mmol/L), did not affect the viability of VSMCs (percentage of viable cells: control 90.9±1.1%, hypoxia 93.1±0.1%, $CoCl_2$ 92.7±1.0%, DMOG 92.5±1.8%; *P* value not significant; n=4).

To examine whether the suppressive effects of hypoxia, $CoCl_2$, and DMOG on vascular AT_1R expression are indeed mediated by PHD inhibition, *Phd* gene expression was knocked down by siRNA introduction. There are at least 3 PHD isoforms. PHD2, however, is believed to play a pivotal role, because PHD2 is broadly expressed in essentially all of the tissues examined,[14–16] and PHD2 knockout results in embryonic lethality.[17] Knockdown of PHD2 (Figure 2A and 2B) downregulated AT_1R protein expression (Figure 2C), indicating that at least PHD2 is involved in PHD inhibition-induced AT_1R downregulation. PHD2 knockdown by siRNA increased nuclear HIF-1α expression (Figure S1B) and mRNA expression of VEGF and phosphoglycerate kinase 1 (Figure S6), of which expression depends on HIF-1, indicating that downregulation of PHD2 by siRNA inhibited PHD2 activity and activated HIF-1. Because hypoxia mimetics are useful to study dose- and time-dependent effects of PHD inhibition on AT_1R expression and can be used for in vivo study, we used hypoxia mimetics in the following experiments.

$CoCl_2$ Inhibited AT_1R mRNA Expression Through Transcriptional and Posttranscriptional Mechanisms

The effect of $CoCl_2$ on AT_1R gene promoter activity was examined. $CoCl_2$ suppressed the AT_1R gene promoter activity in a dose-dependent manner (Figure 3A). The data suggest that $CoCl_2$ suppresses AT_1R gene expression at the transcriptional level.

Next, the deletion mutants of AT_1R gene promoter/luciferase fusion DNA were used to locate the specific DNA element responsible for $CoCl_2$-induced AT_1R suppression. The luciferase activity was suppressed in all of the mutants, suggesting that the most proximal region of the AT_1R gene promoter is critical for downregulation by $CoCl_2$ (Figure 3B).

The effect of $CoCl_2$ on AT_1R mRNA stability was examined. $CoCl_2$ enhanced AT_1R mRNA degradation (Figure 3C). The expression level of AT_1R mRNA was reduced to 42.7±2.8% after 12 hours in vehicle-treated cells. In contrast, $CoCl_2$ increased the AT_1R mRNA degradation rate (28.4±4.4% at 12 hours). The data suggest that $CoCl_2$ downregulates AT_1R gene expression through the posttranscriptional mechanism.

Next, we examined whether $CoCl_2$-induced AT_1R mRNA downregulation requires de novo protein synthesis. Incubation with cycloheximide alone for 24 hours upregulated the

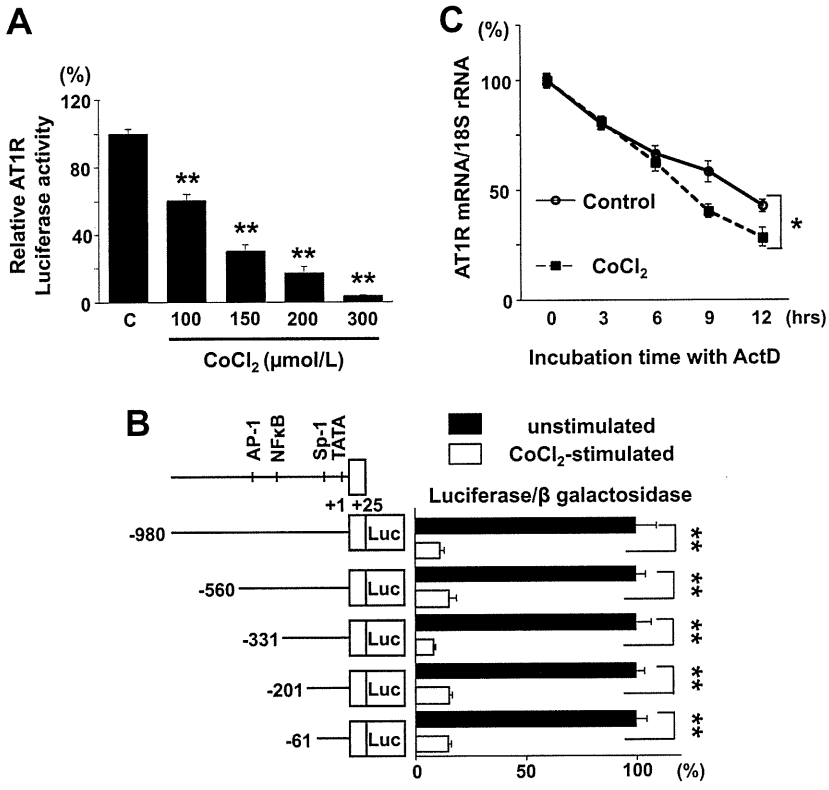

Figure 3. Effect of cobalt chloride ($CoCl_2$) on angiotensin II type 1 receptor (AT_1R) gene promoter activity and mRNA stability in vascular smooth muscle cells (VSMCs). **A** and **B**, AT_1R gene promoter/luciferase DNA construct and LacZ gene were introduced into VSMCs. **A**, VSMCs were stimulated with $CoCl_2$ for 24 hours at varying concentrations as indicated in the Figure. Luciferase activity was normalized by β-galactosidase activity. Relative luciferase activity of control (C) was set as 100%. Data are shown as mean±SEM (n=3). $^{**}P<0.01$ vs C. **B**, The scheme of deletion mutants of AT_1R gene promoter/luciferase fusion DNA construct is shown in the left panel. Relative AT_1R luciferase activity normalized by β-galactosidase activity corresponding to the left luciferase DNA construct is indicated by the bar graph in the right panel. Relative luciferase activity of unstimulated VSMCs in each construct was set as 100%. ■ and □ indicate the relative luciferase activity of unstimulated and $CoCl_2$-stimulated VSMCs, respectively. Values (mean±SEM) are expressed as a percentage of control culture (unstimulated); n=6; $^{**}P<0.01$. **C**, VSMCs were stimulated with $CoCl_2$ (200 μmol/L) for 3 hours. Then actinomycin D (ActD; 5 μg/mL) was added and incubated for the indicated periods. In the control experiment, only ActD was added to the medium. Northern blot analyses were performed as described in the legend to Figure 1. The ratio of AT_1R mRNA/18S rRNA before the ActD addition in each group was designated 100%. Results are expressed as mean±SEM (n=4). $^{*}P<0.05$ vs control (2-way ANOVA).

AT_1R mRNA expression. In the presence of cycloheximide, $CoCl_2$ still significantly suppressed the AT_1R mRNA expression (Figure S7). The data suggest that de novo protein synthesis is not required for $CoCl_2$-induced AT_1R mRNA downregulation.

$CoCl_2$ and PHD2 Knockdown Reduced Cellular Response to Ang II

Ang II is known to induce phosphorylation of ERK in VSMCs through AT_1R.[18] VSMCs were pretreated with $CoCl_2$ (200 μmol/L) for 30 minutes, 24 hours, and 48 hours and then stimulated with Ang II (100 nmol/L) for 5 minutes. Ang II–induced ERK phosphorylation was not affected by 30 minutes of preincubation with $CoCl_2$. ERK phosphorylation was significantly reduced after 24 or 48 hours of preincubation with $CoCl_2$ (Figure 4A). The data suggest that $CoCl_2$-induced AT_1R downregulation results in the attenuation of the cellular response to Ang II. The lack of suppression of Ang II–induced ERK activation after preincubation with $CoCl_2$ for 30 minutes suggests that the direct inhibition of AT_1R signaling by $CoCl_2$ is unlikely. Phorbol-12-myristate-13-acetate–induced ERK phosphorylation was not affected by preincubation with $CoCl_2$, confirming that the ERK activation pathway is not inhibited by $CoCl_2$ (Figure S8). PHD2 knockdown by siRNA also significantly attenuated Ang II–induced ERK phosphorylation (Figure 4B).

PHD Inhibition–Induced AT_1R mRNA Downregulation Was Independent of HIF-1α

To examine whether HIF-1α is involved in PHD inhibition–induced AT_1R mRNA downregulation, the effect of the overexpression of constitutively active HIF-1α on AT_1R mRNA expression was examined. The constitutively active HIF-1α vector was introduced into VSMCs with either the HRE/luciferase construct or the AT_1R gene promoter/luciferase construct. As a control, an empty vector was used. HRE-driven promoter activity was increased significantly by introduction of constitutively active HIF-1α, but AT_1R gene promoter activity was not affected (Figure 5). These data

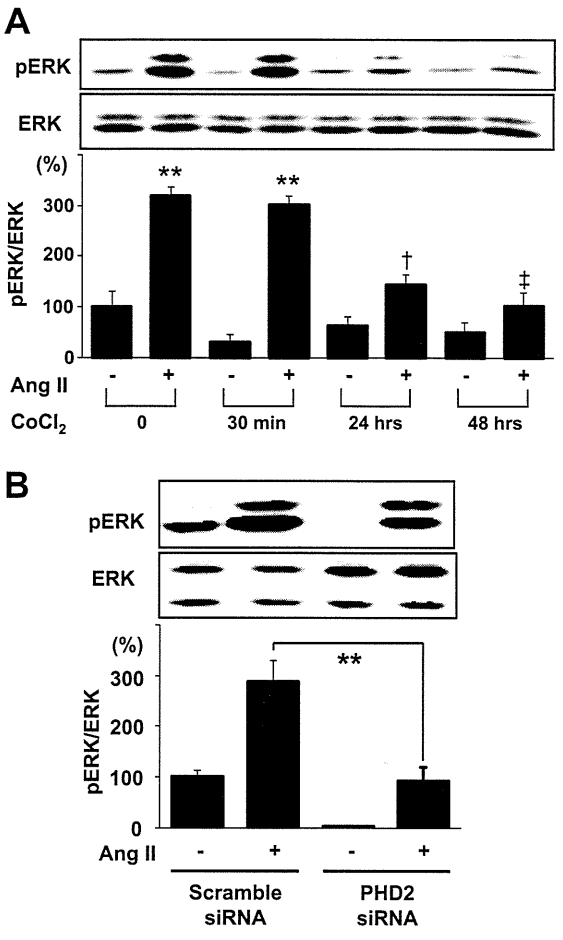

Figure 4. Cobalt chloride ($CoCl_2$) and prolyl hydroxylase domain-containing protein (PHD) 2 knockdown attenuated angiotensin (Ang) II–induced extracellular signal–regulated kinase (ERK) phosphorylation. **A**, Vascular smooth muscle cells (VSMCs) were pretreated with $CoCl_2$ (200 μmol/L) for 30 minutes, 24 hours, and 48 hours and then stimulated with Ang II (100 nmol/L) for 5 minutes (n=4). **B**, VSMCs were transfected with scramble small interfering RNA (siRNA) or PHD2-specific siRNA for 72 hours and then stimulated with Ang II (100 nmol/L) for 5 minutes (n=3). Phospho (p)ERK and ERK protein were detected by Western blot analysis. The ratio of pERK/ERK is shown in the bar graph. Values (mean±SEM) are expressed as a percentage of control culture or scramble siRNA (100%). $^{**}P<0.01$ vs Ang II (−) at time 0 or scramble siRNA and Ang II (+). $\dagger P<0.05$, $\ddagger P<0.01$ vs Ang II (+) and $CoCl_2$ (−) at time 0.

suggest that HIF-1α is not involved in PHD inhibition–induced AT_1R mRNA downregulation.

$CoCl_2$ Attenuated the AT_1R Expression in the Aorta and Perivascular Fibrosis of the Coronary Arteries

We examined whether $CoCl_2$ affects the expression of AT_1R in vivo. Systolic blood pressure was elevated in mice receiving Ang II, and $CoCl_2$ did not affect systolic blood pressure level (Table). The expression level of AT_1R protein in the aorta was significantly decreased in mice receiving $CoCl_2$ (Figure 6A). However, expression of renin in the kidney and expression of angiotensin-converting enzyme and Ang II type 2 receptor in the aorta were not affected. Serum concentration of angiotensinogen was not elevated either (Figure S9). Perivascular fibrosis of the small coronary arteries of the heart was increased by Ang II infusion, which was inhibited by $CoCl_2$ treatment (Figure 6B and 6C). In contrast, interstitial fibrosis of the kidney was not reduced by $CoCl_2$ (Figure S10). Medial thickness of the coronary arteries was slightly increased by Ang II. However, the increase was not statistically significant, and we did not observe a significant effect of $CoCl_2$ (data not shown).

Discussion

In the present study, we demonstrated that hypoxia, $CoCl_2$, and DMOG suppressed AT_1R expression in cultured VSMCs. PHD2 knockdown by RNA interference also reduced AT_1R expression in VSMCs. The AT_1R expression was specifically suppressed because VEGF mRNA was upregulated. $CoCl_2$ suppressed AT_1R expression through transcriptional and posttranscriptional mechanisms. $CoCl_2$ and PHD2 knockdown suppressed Ang II–induced ERK phosphorylation in vitro, and $CoCl_2$ attenuated Ang II–induced perivascular fibrosis of the small coronary arteries in vivo.

Cobalt has been reported to attenuate the lesion formation in many experimental animal models, including renal ischemic injury,[19] myocardial ischemia-reperfusion injury,[20] and cerebral ischemia,[21] in which activation of RAS is involved in the development of these lesions. Because AT_1R expression was downregulated by $CoCl_2$, we suppose that suppression of Ang II–induced perivascular fibrosis of the coronary arteries in this study and attenuation of ischemic injury in previous studies by $CoCl_2$[19–21] might be ascribed, at least in part, to inhibition of AT_1R expression. It is interesting that Ang II–induced renal interstitial fibrosis was not affected by $CoCl_2$. This may suggest that renal interstitial fibrosis is more dependent on blood pressure that was not affected by $CoCl_2$.

We showed a direct inhibitory effect of $CoCl_2$ on AT_1R expression in VSMCs. However, our study could not exclude the possible indirect effects of $CoCl_2$ on the Ang II signaling in vivo. Recent studies showed that inhibition of PHD, using different PHD inhibitors, lowered the levels of proinflammatory cytokines, such as tumor necrosis factor-α, in different models.[22–24] Tumor necrosis factor-α and interleukin 1β have been reported to transcriptionally enhance the AT_1R gene expression in cardiac fibroblasts.[25–27] Therefore, reduction of Ang II–induced cytokine production may also be responsible for $CoCl_2$-induced AT_1R downregulation in vivo.

It is interesting that Ang II alone did not affect AT_1R expression in the aorta, although Ang II is known to suppress AT_1R in VSMCs,[28] which is designated homologous downregulation. The lack of homologous downregulation may also be explained by compensation by Ang II–induced cytokines that upregulate AT_1R as described above.[25–27]

$CoCl_2$ is known to inhibit PHD activity and increase HIF-1 level.[13] Several mechanisms for PHD inhibition by $CoCl_2$ have been suggested.[29] The most likely mechanism is that Co^{2+} substitutes for Fe^{2+}, the cofactor directly required for PHD catalytic activities.[30] Another proposed mechanism is that cobalt produces reactive oxygen species, which inactivate the PHD either directly or indirectly by depleting

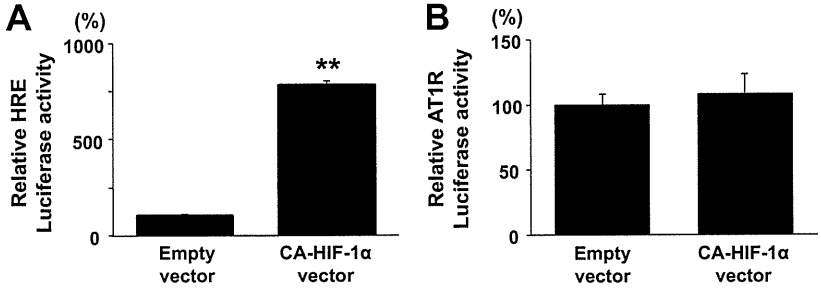

Figure 5. Effect of overexpression of constitutively active (CA) Hypoxia-inducible factor 1α (HIF-1α) on angiotensin II type 1 receptor (AT$_1$R) mRNA expression in vascular smooth muscle cells (VSMCs). **A** and **B**, VSMCs were transfected with CA-HIF-1α vector and either the hypoxia response element (HRE)/luciferase construct or the AT$_1$R gene promoter/luciferase construct. HRE-driven promoter and AT$_1$R gene promoter activities were measured after 48 hours of the transfection, as described in the legend to Figure 3. As a control, an empty vector was used instead of CA-HIF-1α. Values (mean±SEM) are expressed as a percentage of control culture (empty vector, n=3 each). **P<0.01 vs empty vector.

ascorbate, which is essential for the regeneration of Fe^{2+} from Fe^{3+} after a hydroxylation reaction.[31]

Because PHD is a negative regulator for HIF-1 expression, we expected that increased HIF-1 may be responsible for the AT$_1$R downregulation. In this study, however, overexpression of the constitutively active HIF-1α did not affect the AT$_1$R gene promoter activity, although it strongly activated HRE-dependent transcription as expected. HRE does not exist in the AT$_1$R gene promoter region, which also suggests that PHD inhibition-induced AT$_1$R downregulation is independent of HIF-1. Therefore, PHD inhibition may induce a transcription repressor or inhibit the transcription factor that activates AT$_1$R gene expression. Further study is needed to clarify this point.

The circulating RAS has been reported to be activated by hypoxia.[7] It was also reported that AT$_1$R mRNA in VSMCs was upregulated under hypoxia (3% O_2, 24 hours).[32] However, in the present study, both AT$_1$R mRNA and protein were downregulated under hypoxia (1% O_2, 24 hours). Although it is possible that the different oxygen concentration may affect the result, the reason for this discrepancy between the present study and the previous one is not clear at this time. We showed that several hypoxia mimetics and PHD2 downregulation suppressed AT$_1$R expression. Therefore, it is plausible to assume that PHD inhibition, possibly including hypoxia, negatively regulates AT$_1$R expression. Our results may also indicate that AT$_1$R downregulation by PHD inhibition under hypoxia antagonizes the circulating RAS activation.

Table. Body Weight, Heart Rate, and Systolic Blood Pressure of Mice

Groups	BW, g	HR, bpm	SBP, mm Hg
Control	24.9±0.4	553±21	102±1
Ang II	25.8±0.2	600±23	128±3*
$CoCl_2$	25.0±0.4	535±13	100±3
Ang II+$CoCl_2$	25.5±0.3	582±21	123±2*

BW indicates body weight; HR, heart rate; SBP, systolic blood pressure; $CoCl_2$, cobalt chloride; Ang II, angiotensin II. BW, HR, and SBP were recorded in mice 4 wk after administration of $CoCl_2$ and infusion of Ang II. Data are expressed as mean±SEM.

*P<0.05 vs control, n=5 to 6 in each group.

The limitation of this study is that we used chemical inhibitor $CoCl_2$ to inhibit PHD. We cannot completely exclude the possible nonspecific effects. However, $CoCl_2$ increased nuclear HIF-1α expression and VEGF mRNA, suggesting that it inhibited PHD and stabilized HIF-1. In addition, hypoxia and DMOG also suppressed AT$_1$R expression (Figures 1A, 1B, S4A, and S4B). Knockdown of PHD2 also resulted in AT$_1$R downregulation (Figure 2). Therefore, we suppose that PHD inhibitors suppress AT$_1$R expression, at least in part, via PHD2 inhibition. However, it is not clear how PHD regulates AT$_1$R gene expression. Sp1 consensus sequence and TATA box are located in the proximal promoter region of the AT$_1$R gene. So far, it has never been reported that activity of Sp1 or TATA box binding protein is regulated by hydroxylation. Further study is needed to determine the PHD regulation of AT$_1$R gene expression.

In the present study, $CoCl_2$ reduced AT$_1$R in aorta and diminished Ang II–induced perivascular fibrosis but it did not affect Ang II–induced hypertension. Although the mechanism remains uncertain, it is known that the nondepressor dose of angiotensin receptor blocker is effective for the inhibition of perivascular fibrosis or cardiac hypertrophy induced by pressure-overload.[33] These data suggest that cardioprotection by angiotensin receptor blocker or AT$_1$R downregulation might be independent of the blood pressure–lowering effect, at least in terms of Ang II–induced fibrosis.

Perspectives

In summary, we demonstrated in the present study that PHD inhibition downregulates AT$_1$R expression, reduces the cellular response to Ang II, and attenuates the profibrotic effect of Ang II on the coronary arteries. Although further studies are required to determine the detailed molecular mechanism for AT$_1$R downregulation, PHD inhibition may be beneficial for the treatment of cardiovascular diseases, in which activation of RAS plays a critical role.

Acknowledgments

We acknowledge the technical expertise of the Support Center for Education and Research, Kyushu University.

Sources of Funding

This study was supported in part by Grants-in-Aid for Scientific Research from the Ministry of Education, Culture, Sports, Science,

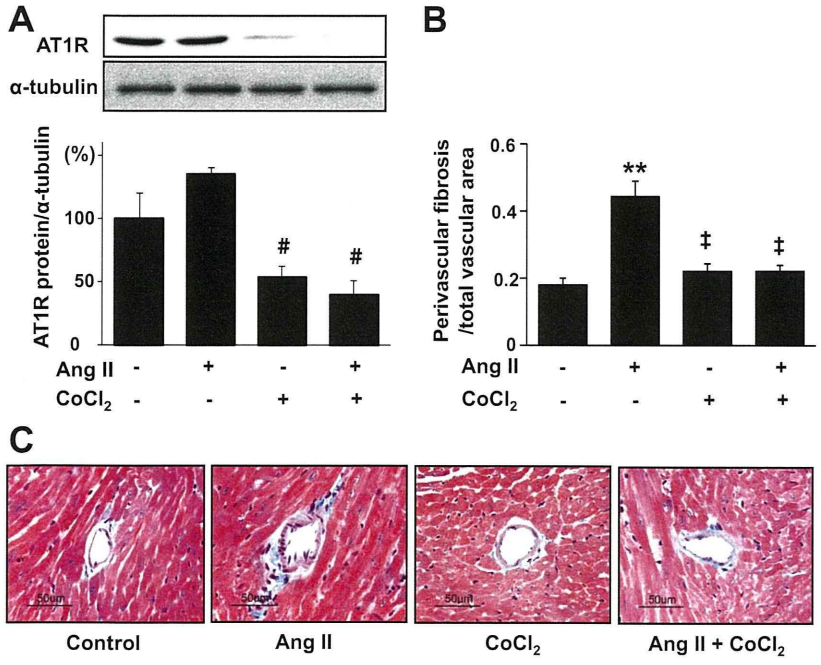

Figure 6. Cobalt chloride ($CoCl_2$) decreased aortic angiotensin II type 1 receptor (AT_1R) expression and attenuated perivascular fibrosis of the coronary arteries in mice. Angiotensin II (Ang II) was intraperitoneally infused through an osmotic minipump. $CoCl_2$ was administered ad libitum in drinking water (0.01%). **A**, After 4 weeks of administration, AT_1R and α-tubulin expression in the aorta was determined by Western blot analysis. The ratio of AT1R/α-tubulin is shown in the bar graph (n=5 to 6, each group). $P<0.05$ vs Ang II (−) and $CoCl_2$ (−). **B**, Perivascular fibrosis of the coronary arteries was examined. Ang II significantly increased perivascular fibrosis of the coronary arteries. $CoCl_2$ inhibited the Ang II–induced perivascular fibrosis (n=5 to 6, each group). $^{**}P<0.01$ vs Ang II (−) and $CoCl_2$ (−). ‡$P<0.01$ vs Ang II (+) and $CoCl_2$ (−). **C**, Representative microphotographs of Masson trichrome-stained mice coronary arteries from each group are shown (n=5 to 6, each group).

and Technology of Japan (19590867 to T.I. and 21790731 to K.T.) and Mitsubishi Pharma Research Foundation for Research Award on Cardiology (2008) to K.T.

Disclosures

None.

References

1. Peach MJ. Renin-angiotensin system: biochemistry and mechanisms of action. *Physiol Rev*. 1977;57:313–370.
2. Dzau VJ, Antman EM, Black HR, Hayes DL, Manson JE, Plutzky J, Popma JJ, Stevenson W. The cardiovascular disease continuum validated: clinical evidence of improved patient outcomes: part I–pathophysiology and clinical trial evidence (risk factors through stable coronary artery disease). *Circulation*. 2006;114:2850–2870.
3. Touyz RM. Reactive oxygen species as mediators of calcium signaling by angiotensin II: implications in vascular physiology and pathophysiology. *Antioxid Redox Signal*. 2005;7:1302–1314.
4. Sasaki K, Yamano Y, Bardhan S, Iwai N, Murray JJ, Hasegawa M, Matsuda Y, Inagami T. Cloning and expression of a complementary DNA encoding a bovine adrenal angiotensin II type-1 receptor. *Nature*. 1991; 351:230–233.
5. Kambayashi Y, Bardhan S, Takahashi K, Tsuzuki S, Inui H, Hamakubo T, Inagami T. Molecular cloning of a novel angiotensin II receptor isoform involved in phosphotyrosine phosphatase inhibition. *J Biol Chem*. 1993;268:24543–24546.
6. Dzau VJ, Antman EM, Black HR, Hayes DL, Manson JE, Plutzky J, Popma JJ, Stevenson W. The cardiovascular disease continuum validated: clinical evidence of improved patient outcomes: part II–clinical trial evidence (acute coronary syndromes through renal disease) and future directions. *Circulation*. 2006;114:2871–2891.
7. Hubloue I, Rondelet B, Kerbaul F, Biarent D, Milani GM, Staroukine M, Bergmann P, Naeije R, Leeman M. Endogenous angiotensin II in the regulation of hypoxic pulmonary vasoconstriction in anaesthetized dogs. *Crit Care*. 2004;8:R163–R171.
8. Kramer BK, Ritthaler T, Schweda F, Kees F, Schricker K, Holmer SR, Kurtz A. Effects of hypoxia on renin secretion and renal renin gene expression. *Kidney Int Suppl*. 1998;67:S155–S158.
9. Semenza GL. HIF-1, O(2), and the 3 PHDs: how animal cells signal hypoxia to the nucleus. *Cell*. 2001;107:1–3.
10. Jiang BH, Rue E, Wang GL, Roe R, Semenza GL. Dimerization, DNA binding, and transactivation properties of hypoxia-inducible factor 1. *J Biol Chem*. 1996;271:17771–17778.
11. Huang LE, Gu J, Schau M, Bunn HF. Regulation of hypoxia-inducible factor 1α is mediated by an O2-dependent degradation domain via the ubiquitin-proteasome pathway. *Proc Natl Acad Sci U S A*. 1998;95: 7987–7992.
12. Berra E, Benizri E, Ginouves A, Volmat V, Roux D, Pouyssegur J. HIF prolyl-hydroxylase 2 is the key oxygen sensor setting low steady-state levels of HIF-1α in normoxia. *Embo J*. 2003;22:4082–4090.
13. Fraisl P, Aragones J, Carmeliet P. Inhibition of oxygen sensors as a therapeutic strategy for ischaemic and inflammatory disease. *Nat Rev Drug Discov*. 2009;8:139–152.
14. Hirsila M, Koivunen P, Gunzler V, Kivirikko KI, Myllyharju J. Characterization of the human prolyl 4-hydroxylases that modify the hypoxia-inducible factor. *J Biol Chem*. 2003;278:30772–30780.
15. Oehme F, Ellinghaus P, Kolkhof P, Smith TJ, Ramakrishnan S, Hutter J, Schramm M, Flamme I. Overexpression of PH-4, a novel putative proline 4-hydroxylase, modulates activity of hypoxia-inducible transcription factors. *Biochem Biophys Res Commun*. 2002;296:343–349.
16. Lieb ME, Menzies K, Moschella MC, Ni R, Taubman MB. Mammalian EGLN genes have distinct patterns of mRNA expression and regulation. *Biochem Cell Biol*. 2002;80:421–426.
17. Takeda K, Ho VC, Takeda H, Duan LJ, Nagy A, Fong GH. Placental but not heart defects are associated with elevated hypoxia-inducible factor αlevels in mice lacking prolyl hydroxylase domain protein 2. *Mol Cell Biol*. 2006;26:8336–8346.
18. Eguchi S, Matsumoto T, Motley ED, Utsunomiya H, Inagami T. Identification of an essential signaling cascade for mitogen-activated protein kinase activation by angiotensin II in cultured rat vascular smooth muscle cells. Possible requirement of Gq-mediated p21ras activation coupled to a Ca2+/calmodulin-sensitive tyrosine kinase. *J Biol Chem*. 1996;271: 14169–14175.
19. Matsumoto M, Makino Y, Tanaka T, Tanaka H, Ishizaka N, Noiri E, Fujita T, Nangaku M. Induction of renoprotective gene expression by cobalt ameliorates ischemic injury of the kidney in rats. *J Am Soc Nephrol*. 2003;14:1825–1832.
20. Xi L, Taher M, Yin C, Salloum F, Kukreja RC. Cobalt chloride induces delayed cardiac preconditioning in mice through selective activation of HIF-1α and AP-1 and iNOS signaling. *Am J Physiol Heart Circ Physiol*. 2004;287:H2369–H2375.
21. Bergeron M, Gidday JM, Yu AY, Semenza GL, Ferriero DM, Sharp FR. Role of hypoxia-inducible factor-1 in hypoxia-induced ischemic tolerance in neonatal rat brain. *Ann Neurol*. 2000;48:285–296.
22. Cummins EP, Seeballuck F, Keely SJ, Mangan NE, Callanan JJ, Fallon PG, Taylor CT. The hydroxylase inhibitor dimethyloxalylglycine is protective in a murine model of colitis. *Gastroenterology*. 2008;134: 156–165.

23. Robinson A, Keely S, Karhausen J, Gerich ME, Furuta GT, Colgan SP. Mucosal protection by hypoxia-inducible factor prolyl hydroxylase inhibition. *Gastroenterology*. 2008;134:145–155.
24. Takeda K, Ichiki T, Narabayashi E, Inanaga K, Miyazaki R, Hashimoto T, Matsuura H, Ikeda J, Miyata T, Sunagawa K. Inhibition of prolyl hydroxylase domain-containing protein suppressed lipopolysaccharide-induced TNF-α expression. *Arterioscler Thromb Vasc Biol*. 2009;29: 2132–2137.
25. Gurantz D, Cowling RT, Villarreal FJ, Greenberg BH. Tumor necrosis factor-α upregulates angiotensin II type 1 receptors on cardiac fibroblasts. *Circ Res*. 1999;85:272–279.
26. Cowling RT, Gurantz D, Peng J, Dillmann WH, Greenberg BH. Transcription factor NF-kappa B is necessary for up-regulation of type 1 angiotensin II receptor mRNA in rat cardiac fibroblasts treated with tumor necrosis factor-α or interleukin-1β. *J Biol Chem*. 2002;277: 5719–5724.
27. Matsubara H, Kanasaki M, Murasawa S, Tsukaguchi Y, Nio Y, Inada M. Differential gene expression and regulation of angiotensin II receptor subtypes in rat cardiac fibroblasts and cardiomyocytes in culture. *J Clin Invest*. 1994;93:1592–1601.
28. Lassegue B, Alexander RW, Nickenig G, Clark M, Murphy TJ, Griendling KK. Angiotensin II down-regulates the vascular smooth muscle AT1 receptor by transcriptional and post-transcriptional mechanisms: evidence for homologous and heterologous regulation. *Mol Pharmacol*. 1995;48:601–609.
29. Maxwell P, Salnikow K. HIF-1: an oxygen and metal responsive transcription factor. *Cancer Biol Ther*. 2004;3:29–35.
30. Kaelin WG Jr, Ratcliffe PJ. Oxygen sensing by metazoans: the central role of the HIF hydroxylase pathway. *Mol Cell*. 2008;30:393–402.
31. Page EL, Chan DA, Giaccia AJ, Levine M, Richard DE. Hypoxia-inducible factor-1α stabilization in nonhypoxic conditions: role of oxidation and intracellular ascorbate depletion. *Mol Biol Cell*. 2008;19: 86–94.
32. Sodhi CP, Kanwar YS, Sahai A. Hypoxia and high glucose upregulate AT1 receptor expression and potentiate ANG II-induced proliferation in VSM cells. *Am J Physiol Heart Circ Physiol*. 2003;284:H846–H852.
33. Regan CP, Anderson PG, Bishop SP, Berecek KH. Pressure-independent effects of AT1-receptor antagonism on cardiovascular remodeling in aortic-banded rats. *Am J Physiol*. 1997;272:H2131–H2138.

ONLINE SUPPLEMENT

Inhibition of Prolyl Hydroxylase Domain-containing Protein Downregulates Vascular Angiotensin II Type 1 Receptor

Hirohide Matsuura[1)]
Toshihiro Ichiki[1), 2)] *
Jiro Ikeda[1)]
Kotaro Takeda[2)]
Ryohei Miyazaki[1)]
Toru Hashimoto[1)]
Eriko Narabayashi[1)]
Shiro Kitamoto[1), 2)]
Tomotake Tokunou[1)]
Kenji Sunagawa[1)]

Departments of Cardiovascular Medicine[1)] and Advanced Therapeutics for Cardiovascular Diseases[2)], Kyushu University Graduate School of Medical Sciences, Fukuoka, Japan.

*To whom correspondence should be addressed: Toshihiro Ichiki, MD., PhD. Department of Cardiovascular Medicine, Kyushu University Graduate School of Medical Sciences, 3-1-1 Maidashi, Higashi-ku, 812-8582 Fukuoka, Japan.
Tel +81-92-642-6546 Fax +81-92-642-5374
E-mail ichiki@cardiol.med.kyushu-u.ac.jp